



Intestinal activation of pH-sensing receptor OGR1 (GPR68) contributes to fibrogenesis

Hutter, Senta ; van Haaften, Wouter T ; Hünerwadel, Anouk ; Baebler, Katharina ; Herfarth, Neel ; Raselli, Tina ; Mamie, Céline ; Misselwitz, Benjamin ; Rogler, Gerhard ; Weder, Bruce ; Dijkstra, Gerard ; Meier, Chantal Florence ; de Vallière, Cheryl ; Weber, Achim ; Imenez Silva, Pedro H ; Wagner, Carsten A ; Frey-Wagner, Isabelle ; Ruiz, Pedro A ; Hausmann, Martin

Abstract: Background and aims pH-sensing ovarian cancer G-protein coupled receptor-1 (OGR1/GPR68) is regulated by key inflammatory cytokines. Patients suffering from inflammatory bowel diseases (IBD) express increased mucosal levels of OGR1 compared to non-IBD controls. pH-sensing may be relevant for progression of fibrosis, as extra-cellular acidification leads to fibroblast activation and extracellular matrix remodeling. We aimed to determine OGR1 expression in fibrotic lesions in the intestine of Crohn's disease (CD) patients, and the effect of Ogr1 deficiency in fibrogenesis. Methods Human fibrotic and non-fibrotic terminal ileum was obtained from CD patients undergoing ileocecal resection due to stenosis. Gene expression of fibrosis markers and pH-sensing receptors was analyzed. For the initiation of fibrosis in vivo, spontaneous colitis by Il10^{-/-}, dextran sodium sulfate (DSS)-induced chronic colitis and the heterotopic intestinal transplantation model were used. Results Increased expression of fibrosis markers was accompanied by an increase of OGR1 (2.71 ± 0.69 vs. 1.18 ± 0.03 , $P=0.016$) in fibrosis-affected human terminal ileum, compared to the non-fibrotic resection margin. Positive correlation between OGR1 expression and pro-fibrotic cytokines (TGFB1 and CTGF) and pro-collagens was observed. The heterotopic animal model for intestinal fibrosis transplanted with terminal ileum from Ogr1^{-/-} mice showed a decrease in mRNA expression of fibrosis markers as well as a decrease in collagen layer thickness and hydroxyproline compared to grafts from wildtype mice. Conclusions OGR1 expression correlates with increased expression levels of pro-fibrotic genes and collagen deposition. Ogr1 deficiency is associated with a decrease in fibrosis formation. Targeting OGR1 may be a potential new treatment option for IBD-associated fibrosis.

DOI: <https://doi.org/10.1093/ecco-jcc/jjy118>

Posted at the Zurich Open Repository and Archive, University of Zurich

ZORA URL: <https://doi.org/10.5167/uzh-157615>

Journal Article

Accepted Version

Originally published at:

Hutter, Senta; van Haaften, Wouter T; Hünerwadel, Anouk; Baebler, Katharina; Herfarth, Neel; Raselli, Tina; Mamie, Céline; Misselwitz, Benjamin; Rogler, Gerhard; Weder, Bruce; Dijkstra, Gerard; Meier, Chantal Florence; de Vallière, Cheryl; Weber, Achim; Imenez Silva, Pedro H; Wagner, Carsten A; Frey-Wagner, Isabelle; Ruiz, Pedro A; Hausmann, Martin (2018). Intestinal activation of pH-sensing receptor OGR1 (GPR68) contributes to fibrogenesis. *Journal of Crohn's Colitis*, 12(11):1348-1358.

DOI: <https://doi.org/10.1093/ecco-jcc/jjy118>

TITLE PAGE**Intestinal acidification sensed by pH-sensing receptor OGR1 (GPR68)
contributes to fibrogenesis**

Short title: Decreased fibrogenesis upon OGR1 depletion

**Senta Hutter^{1#}, Wouter Tobias van Haaften^{2,3#}, Anouk Hünérwadel¹,
Katharina Baebler¹, Neel Herfarth¹, Tina Raselli¹, Céline Mamie¹, Benjamin
Misselwitz¹, Gerhard Rogler^{1,4}, Bruce Weder¹, Gerard Dijkstra², Chantal
Florence Meier¹, Cheryl de Vallière¹, Achim Weber⁵, Carsten A. Wagner⁴,
Isabelle Frey-Wagner¹, Pedro A. Ruiz¹, Martin Hausmann¹**

¹ Department of Gastroenterology and Hepatology, University Hospital Zürich,
Zürich, Switzerland

² Department of Gastroenterology and Hepatology, University Medical Center
Groningen, University of Groningen, Groningen, the Netherlands

³ Department of Pharmaceutical Technology and Biopharmacy, Groningen
Research Institute of Pharmacy, University of Groningen, Groningen, The
Netherlands

⁴ Institute of Physiology, University of Zürich, Zürich, Switzerland

⁵ Department of Pathology and Molecular Pathology, University Hospital Zürich,
Zürich, Switzerland

Equal contribution

Corresponding author:

Martin Hausmann PhD

Department of Gastroenterology and Hepatology

University Hospital Zürich

8091 Zurich, CH-Switzerland

Mail: martin.hausmann@usz.ch

Tel.: +41 44 255 9916, Fax: +41 44 255 9496

Word count (abstract, main body, references): 5694

Abbreviations:

ACTA2, α -smooth muscle actin; ASMC, airway smooth muscle cells; ACTB, beta-actin; CD, Crohn's disease; CTGF, connective tissue growth factor; ECM, extracellular matrix; GAPDH, glyceraldehyde-3-phosphate dehydrogenase; OGR1/GPR68, G-protein coupled receptor 1; GPR, G-protein-coupled receptor; HSP90, heat shock protein 90; HPRT, hypoxanthine phosphoribosyltransferase 1; HYP, 4-Hydroxyproline; IBD, inflammatory bowel diseases; IL, interleukin; MSC, mesenchymal stem cell; mRNA, messenger RNA; COL1A1, pro-collagen type I alpha 1; COL3A1, pro-collagen type III alpha 1; RT-qPCR, quantitative reverse-transcription polymerase chain reaction; TDAG8/GPR65, T cell death-associated gene 8; TGF- β 1, Transforming growth factor β 1; TNF, tumor necrosis factor; UC, ulcerative colitis; VIM, vimentin

No external writing assistance was provided in drafting this manuscript

The manuscript, including related data, figures and tables has not been
previously published and that the manuscript is not under consideration
elsewhere

Authors contributions

- study concept; G Rogler
- acquisition of data and drafting of the manuscript; S Hutter, WT van Haaften, M Hausmann
- acquisition of data: A Hünerwadel, C Mamie, B Weder, CF Meier, K Baebler, N Herfarth
- critical revision of the manuscript; B Misselwitz, G Rogler, G Dijkstra, C de Vallière, A Weber, C Wagner, I Frey-Wagner, PA Ruiz, M Hausmann
- technical support; C Mamie, T Raselli
- all authors approved the final submitted version of the manuscript

ABSTRACT

Background and aims: pH-sensing ovarian cancer G-protein coupled receptor-1 (OGR1/GPR68) is regulated by key inflammatory cytokines. Patients suffering from inflammatory bowel diseases (IBD) express increased mucosal levels of OGR1 in the mucosa compared to non-IBD controls. pH-sensing may be relevant for progression of fibrosis, as extra-cellular acidification leads to fibroblast activation and extracellular matrix remodeling. We aimed to determine *OGR1* expression in fibrotic lesions in the intestine of Crohn's disease (CD) patients, and the effect of *Ogr1* deficiency in fibrogenesis.

Methods: Human fibrotic and non-fibrotic terminal ileum was obtained from CD patients undergoing ileocecal resection due to stenosis. Gene expression of fibrosis markers and pH-sensing receptors was analyzed. The *in vivo* murine heterotopic transplantation model of intestinal fibrosis was used. Collagen layer thickness and hydroxyproline content was determined.

Results: Increased expression of fibrosis markers was accompanied by an increase of *OGR1* (2.71 ± 0.69 vs. 1.18 ± 0.03 , $P=0.016$) in fibrosis-affected human terminal ileum, compared to the non-fibrotic resection margin. Positive correlation between *OGR1* expression and pro-fibrotic cytokines (*TGFB1* and *CTGF*) or pro-collagens was observed. The heterotopic animal model for intestinal fibrosis transplanted with terminal ileum from *Ogr1*^{-/-} mice showed a significant decrease in mRNA expression of fibrosis markers as well as a decrease in collagen layer thickness and hydroxyproline compared to grafts from wildtype mice.

Conclusions: *OGR1* expression correlates with the expression of pro-fibrotic genes and increased levels of collagen deposition. *Ogr1* deficiency is

89 associated with a decrease in fibrosis formation. Targeting OGR1 may be a
90 potential new treatment option for IBD-associated fibrosis.

91

92 **Keywords:** Fibrosis, Crohn's disease, IBD models

INTRODUCTION

Recent studies have shown a link between inflammatory bowel diseases (IBD) and the family of pH-sensing G-protein-coupled receptors (GPRs).¹⁻⁵ Three GPRs from the GPR4-subfamily were identified as sentinels for proton concentration, as they enable cells to sense the surrounding pH and to respond to it.^{6, 7} This GPR4-subfamily of receptors includes GPR4, ovarian cancer GPR 1 (OGR1/GPR68) and T cell death-associated gene 8 (TDAG8/GPR65). These receptors sense extracellular protons through histidine residues located in the extracellular region of the receptors, resulting in signaling pathway activation and the modification of a variety of cell functions.^{6, 7} GPRs are also regulated by key inflammatory cytokines.⁸⁻¹⁰ The proton-sensing pH receptors TDAG8, OGR1 and GPR4 are inactive or only slightly active in an alkaline environment (pH 7.6-7.8), but become highly activated in acidic environments (pH 6.8).^{7, 11-13} GPR132 structurally belongs to the subclade but is not considered anymore as a true member of this family.

IBD affects approximately one in a hundred and fifty people in the industrialized world. It comprises two main conditions, namely ulcerative colitis (UC) and Crohn's disease (CD), and is characterized by a chronic inflammation of the intestinal wall. Severe and persistent mucosal tissue damage is one of the main features of IBD. Tissue injury is associated with an acidic pH shift, as inflammation increases local proton concentration and lactate production. This induces subsequent pro-inflammatory cytokine production, such as tumor necrosis factor (TNF).¹⁴⁻¹⁶ An acidic environment is not only the result of inflammation but also affects the degree and outcome of inflammation.^{13, 17, 18} A disturbed pH homeostasis due to acidification of the intestinal environment

leads to the activation of OGR1.¹⁹ Recent work demonstrates that patients suffering from IBD express increased levels of *OGR1* in the mucosa compared to non-IBD controls.^{3, 4} The expression of *OGR1* is also increased in inflamed colonic mucosa compared to non-inflamed colonic mucosa in both CD and UC patients. Moreover, in mice lacking *Ogr1*, inflammation was attenuated.⁴

Wound healing after tissue damage requires an exquisite balance between multiple pro- and anti-fibrotic stimuli on extracellular matrix (ECM)-producing cells²⁰⁻²³ e.g. activated myofibroblasts.²⁴ Matrix-producing cells are activated by paracrine signals, autocrine factors, damage-associated molecular patterns or pathogen-associated molecular patterns derived from microorganisms.²⁵⁻²⁸

Transforming growth factor β 1 (TGF- β 1) is an important mediator of mesenchymal cell activation and its expression is increased in inflamed mucosa of IBD patients.²⁹⁻³² Excessive tissue repair promotes fibrosis, impairs gastrointestinal function, and is a common clinical problem in patients with CD and UC.³³ Increased tissue stiffness is associated with impaired absorption upon fibrogenesis.²⁸ Fibrosis is increasingly recognized as an important cause of morbidity and mortality in patients with IBD. Intestinal fibrosis leads to stricture formation due to thickening of the intestinal wall in 30-50% of patients with CD,^{34, 35} and approximately 80% of these patients will require surgery.³⁴

Recently, it has been shown that fibrogenesis can also occur in long-standing (≥ 10 years) UC, leading to the formation of strictures.³⁶

In this study, we determined the expression of *OGR1* in fibrotic lesions of human intestine in patients with CD compared to non-fibrotic control sections. Our results show that *OGR1* expression correlates with the expression of pro-fibrotic genes and the levels of collagen deposition. Furthermore, we studied

143 the role of *Ogr1* in intestinal fibrogenesis in an animal model of fibrosis. Our
144 results show that *Ogr1* deficiency is associated with a decrease in fibrosis
145 formation. Targeting OGR1 may be a potential new treatment option for IBD-
146 associated fibrosis.

MATERIALS AND METHODS

Human tissue from patients with CD and non-fibrotic control patients

Intestinal tissue from patients with CD was obtained from patients undergoing ileocecal resection because of stenosis in the terminal ileum (non-fibrosis affected resection margin and from the thickened fibrosis-affected region), and from patients undergoing right-sided hemicolectomy because of an adenocarcinoma (non-cancer affected ileal resection margin, Supplementary table 1). Just after resection, samples for RNA were fixed in Tissue-Tek® (O.C.T. Compound, Sakura® Finetek) in the operation room and frozen in isopentane on dry ice. Samples were stored at -80°C until further use. Intestinal epithelial crypts were isolated as previously described.³⁷

Animals

All animal experiments were performed according to the ARRIVE criteria for *in vivo* experiments. The generation, breeding and genotyping of male C57BL/6J-*Ogr1*^{tm1} (*Ogr1*^{-/-}) has been described previously.^{4, 19} The animals were co-housed to minimize potential effects of different microbiota. Male C57BL/6 wildtype (WT) donor mice were obtained from Jackson Laboratories. 12 female B6-Tg(UBC-GFP)30Scha/J (GFP) recipient mice were bred locally. Mice used for the experiment weighed 19-23 g and were 12-16 weeks old when the experiment was started. The animals received standard laboratory mouse food and water *ad libitum*. They were housed under specific pathogen-free conditions in a regular day-night cycle in individually ventilated cages with standard bedding and cage enrichment. Surgeries were always performed during the light cycle.

Ethical considerations

Patients gave written informed consent for anonymous use of patient data and resected parts of human intestine according to the code of conduct for responsible use of surgical left-over material (See: Code goed gebruik voor gecodeerd lichaamsmateriaal, Research Code University Medical Center Groningen, (www.rug.nl/umcg/research/documents/research-code-info-umcg-nl.pdf)). Further, we retrieved permission to isolate different mucosal cells from intestinal samples, and to use data from patients from a cohort study of Swiss residents diagnosed with IBD, approved by the local ethical committee of the Kanton Zurich (EK-1316). The animal experiment protocol was approved by the Veterinary Authority of the Kanton of Zurich (registration number ZH242/2016).

Heterotopic intestinal transplant model

The heterotopic mouse intestinal transplant model is an adaption of the heterotopic transplantation model of intestinal fibrosis in rats, which has been previously described in detail.³⁸ Briefly, donor small bowel resections were extracted and transplanted subcutaneously into the neck of recipient animals. Donor small bowel proximal to the caecum was excised and flushed with 5 ml of 0.9 % NaCl to remove stool, and divided into 10 mm parts. A small bowel resection was implanted into a subcutaneous pouch, and a single dose of Cefazolin (Kefzol®, 1g diluted in 2.5ml distilled water) was administered intraperitoneally as infection prophylaxis. Intestinal grafts were explanted 7 days after transplantation. Donor and recipient mice were euthanized by cervical dislocation. After explantation, each graft was divided into three equal

segments. One segment was fixed in 4 % formalin for histopathological assessment. The other two segments were snap frozen in liquid nitrogen and stored at -80° C until RNA extraction or for determination of hydroxoproline (HYP) content.

RNA isolation and RT-qPCR from Tissue-Tek embedded samples and from mouse samples

For human samples, ten 10 µM thick Tissue-Tek sections, containing full cross sections of the intestinal wall were cut using a cryostat. Sections were dissolved and homogenized in TRIzol (Invitrogen, Life Technologies) and total RNA was isolated according to the manufacturer's protocol. To avoid genomic DNA contamination, samples were treated with DNase I, Amp Grade (Invitrogen, Life Technologies) according to the manufacturer's protocol. RNA isolation from mucosa, crypts and epithelial cells was performed as previously described.³⁷ RNA isolation of mice specimens was performed following the instructions of the RNeasy Mini Kit (Qiagen). RT-qPCR was performed using TaqMan gene expression assays (Supplementary table 2). mRNA expression is presented as $2^{-\Delta Ct}$, normalized to one of the samples in the control group.

Sirius Red staining and collagen layer thickness measurement

Fixed samples were processed in a benchtop tissue processor (Leica TP 1020), embedded and cut into 3µm sections. To visualize the collagen layer, the samples were stained with Sirius Red according to a standard protocol.³⁹ Sirius red staining was examined using the Imager Z2 microscope (Zeiss) and the software AxioVision (Zeiss). The quantity of the by Sirius red stained collagen

was analyzed by ImageJ 1.47t (NIH, USA) using pictures taken under transmission light, as well as using a polarized light filter. To quantify the area with Sirius red stained collagen, cropped 100-fold magnification pictures (length:width ratio = 3:1) from at least eight representative areas comprising the collagen layer broad wise, for each single graft were taken. By setting thresholds to select the red collagen using ImageJ, the area being covered with collagen was quantified. Additionally, collagen layer thickness was measured in μm by a blinded investigator from at least eight places of representative areas at 100-fold magnification.

4-Hydroxyproline (HYP) assay

HYP (a major component of collagen) content was quantified from freshly isolated small bowel and grafts using a HYP assay (MAK008-1KT, Sigma-Aldrich) according to the manufacturer's protocol. In brief, tissues (10–30mg) were homogenized using gentleMACS Octo Dissociator (130-096-427, Miltenyl Biotec) and hydrolyzed in 12M HCl (10 $\mu\text{L}/\text{mg}$ tissue). The hydrolysate was transferred in duplicates to a 96 well plate and dried at 60°C. Dried samples were incubated with 50 μL of chloramine T/oxidation buffer mixture (3 μL of the chloramine T concentrate and 47 μL of the oxidation buffer) at room temperature for 5 minutes. 50 μL of the diluted DMAB reagent (25 μL dimethylaminobenzaldehyde, 25 μL perchloric acid/isopropanol) was added and samples were incubated at 60 °C for 90 minutes for chromophore formation. Absorbance was measured at 560nm.

Statistical analysis

GraphPad Prism software (v5.0) was used. All human RT-qPCR data was considered non-parametric. Therefore, non-paired analyses were performed using the Mann-Whitney U test, and paired analyses were performed using a Wilcoxon matched-pairs signed rank test. If more than 2 groups were compared, a Kruskal-Wallis with post-hoc Dunn's test for multiple comparisons was performed. Correlation was determined using Spearman's rank correlation coefficient.

Mouse data was considered parametric. Therefore, statistical analysis for collagen layer thickness was performed using one-way analysis of variance on ranks, all pairwise multiple comparison procedures (Student Newman-Keuls method). Statistical analysis for the HYP assay was performed using unpaired t-test. Statistical analysis for RT-qPCR in mice was performed using unpaired t-test or one-way analysis of variance on ranks, all pairwise multiple comparison procedures (Student Newman-Keuls method).

Differences were considered significant at a *P*-value of <0.05* and highly significant at a *P*-value of <0.01** and *P*-value of <0.001***. In text and figures, averages \pm standard error of the mean are presented.

RESULTS

Expression of pH-sensing G-protein coupled receptors is increased in the fibrotic intestine in CD patients

To elucidate the pathophysiological relevance of pH-sensing receptors, we determined whether the expression of GPRs is increased in fibrosis affected terminal ileum vs. non-fibrotic terminal ileum from patients with CD. mRNA expression of fibrosis markers *COL1A1* (108.46 ± 60.57 vs. 6.70 ± 2.02 , $*P < 0.05$), *COL3A1* (35.68 ± 17.66 vs. 3.14 ± 0.73 , $*P < 0.05$), *ACTA2* (13.91 ± 4.10 vs. 5.12 ± 2.20 , $*P < 0.05$) and *TGFB1* (4.72 ± 1.18 vs. 1.52 ± 0.34 , $**P < 0.01$) was significantly increased in the fibrosis-affected area, compared to the non-fibrosis affected resection margin (Figure 1A). The increase of fibrosis markers was accompanied by a significant increase in the mRNA expression of *OGR1* (*GPR68*, 2.71 ± 0.69 vs. 1.18 ± 0.03 , $*P < 0.05$), *TDAG8* (*GPR65*, 4.14 ± 1.01 vs. 1.59 ± 0.32 , $**P < 0.01$) and *GPR4* (9.94 ± 1.05 vs. 3.23 ± 0.76 , $*P < 0.05$) in the fibrosis-affected terminal ileum (Figure 1B). For *GPR132* (1.28 ± 0.38 vs. 0.64 ± 0.12 , $P = 0.08$), no difference between fibrosis and non-fibrosis affected tissue was observed. To verify that the (unaffected) resection margins were free of fibrosis, we compared these samples to non-cancer affected terminal ileum resection margins from resections due to adenocarcinoma. Here, no differences were observed in mRNA expression of *COL1A1* (6.70 ± 2.01 vs. 2.07 ± 0.50 , $P = 0.57$), *COL3A1* (3.14 ± 0.72 vs. 1.26 ± 0.34 , $P = 0.21$), *ACTA2* (5.12 ± 2.20 vs. 2.72 ± 0.40 , $P > 0.99$) and *TGFB1* (1.52 ± 0.44 vs. 1.06 ± 0.42 , $P = 0.68$, Supplementary figure 1). Also, no differences were observed between non-cancer affected control tissue and the non-fibrosis affected resection margin from patients with CD in *OGR1* (*GPR68*, 1.18 ± 0.03 vs. 0.93 ± 0.16 ,

$P=0.57$), *TDAG8* (*GPR65*, 1.59 ± 0.31 vs. 1.41 ± 0.24 , $P=0.81$), *GPR4* (3.24 ± 0.76 vs. 3.73 ± 1.41 , $P=0.57$) and *GPR132* (0.64 ± 0.12 vs. 0.91 ± 0.28 , $P=0.46$, Supplementary figure 1, Supplementary table 2). Furthermore, a correlation between *GPR68* (*OGR1*) vs. *COL3A1* (R^2 0.791, $***P<0.001$) and *TGFB1* (R^2 0.850, $***P<0.001$) was found (Figure 2, Table 1). This confirms our hypothesis that expression of *OGR1* is associated with fibrogenesis in human terminal ileum, affected by CD.

To further examine which cells of the intestinal mucosa express the different pH-sensing receptors, mRNA expression for *GPR68* (*OGR1*), *GPR65* (*TDAG8*), *GPR4*, and *GPR132* was determined in RNA isolated from epithelial cells and mucosa from the same patient sample (Supplementary figure 2). mRNA expression of the pH-sensing GPRs was increased in whole mucosal tissue compared to isolated crypts for *OGR1* (*GPR68*, 15.7 ± 15.0 (n=13) vs. 1.2 ± 2.5 (n=8), $**P<0.01$) *TDAG8* (*GPR65*, 30.6 ± 42.1 (n=12) vs. 0.6 ± 0.8 (n=8), $**P<0.01$), *GPR132* (33.5 ± 40.2 (n=13) vs. 1.3 ± 3.0 (n=8), $**P<0.01$) and *GPR4* (80.3 ± 90.1 (n=13) vs. 7.0 ± 15.1 (n=8), $**P<0.01$, Supplementary figure 2). These results suggest that GPRs are mainly expressed by non-epithelial cells of the lamina propria of the human intestine such as fibroblasts or immune cells.

Expression of pH-sensing receptors increases upon fibrogenesis in mice

To determine the relevance of *OGR1* in the development of fibrosis in murine tissue, *Ogr1*^{-/-} and WT mice were used as donors and GFP expressing mice as recipients for isogeneic transplantation of the intestine in our heterotopic animal model for intestinal fibrosis. Body weight remained unchanged in both GFP recipient groups receiving either *Ogr1*^{-/-} or WT grafts (data not shown). Grafts

were explanted 7 days after transplantation. From the 24 intestinal transplants, histologically evaluable tissue was obtained from all but 5 grafts.

We hypothesized that increased expression of pH-sensing receptor OGR1 plays a role in fibrosis formation in both human and murine intestine. *Ogr1* (*Gpr68*) mRNA expression in intestinal explants from WT donor mice at day 7 after heterotopic transplantation was indeed significantly increased compared to WT donor grafts at day 0 before transplantation (5.71 ± 1.03 (n=7) vs. 1.92 ± 0.72 (n=6) $*P < 0.05$, Figure 3A). Furthermore, expression of *Tdag8* (*Gpr65*) was increased in the grafts at day 7 after heterotopic transplantation compared to freshly isolated small bowel in WT (4.06 ± 1.04 (n=7) vs. 1.56 ± 0.61 (n=6), $*P < 0.05$, Figure 3B). Next to that, *Tdag8* (*Gpr65*) expression was decreased in the *Ogr1*^{-/-} grafts explanted at day 7 compared to WT grafts (2.36 ± 0.45 (n=11) vs. 4.06 ± 1.04 (n=7), $*P < 0.05$, Figure 3B).

Expression of fibrosis markers is decreased in *Ogr1*^{-/-} grafts upon induction of fibrosis

Expression of fibrosis markers *Vim*, *Col3a1*, *Tgfb1* and *Ctgf* was used to confirm the induction of fibrosis in this model and to study the effect of the lack of *Ogr1*. mRNA expression of *Vim*, a mesenchymal cell marker that can be used as a surrogate marker for the number of fibroblasts and the occurrence of endothelial-to-mesenchymal transition (EMT), was increased in WT grafts 7 days after transplantation compared to the small bowel at day 0 (4.94 ± 0.85 (n=7) vs. 0.65 ± 0.08 (n=6), $***P < 0.001$, Figure 4A). Furthermore, mRNA expression of *Col3a1* (395.55 ± 201.0 (n=6) vs. 1.15 ± 0.17 (n=6), $*P < 0.05$), *Tgfb1* (4.75 ± 0.94 (n=7) vs. 0.98 ± 0.17 (n=6), $***P < 0.001$), as well as *Ctgf*

(8.08 ± 2.63 (n=7) vs. 1.70 ± 0.64 (n=5), $*P < 0.05$) was increased in grafts from WT donor mice 7 days after transplantation, showing that fibrosis was adequately induced in this model. mRNA expression of these four markers was not significantly increased in the *Ogr1*^{-/-} grafts 7 days after heterotopic transplantation, compared to the small bowel at day 0 (Figure 4B-D).

Most importantly, mRNA expression of *Vim* was decreased in grafts from *Ogr1*^{-/-} donor mice compared to grafts from WT mice at day 7 after heterotopic transplantation (2.80 ± 0.41 , (n=11) vs. 4.94 ± 0.85 (n=7) $**P < 0.01$, Figure 4A).

The expression of *Col3a1* mRNA was also decreased in *Ogr1*^{-/-} grafts compared to WT mice at day 7 after transplantation (76.55 ± 28.88 (n=11) vs. 395.55 ± 201.0 (n=6) $*p < 0.05$, Figure 4B). Furthermore, mRNA expression of *Tgfb1* and *Ctgf*, two mediators involved in activation of myofibroblasts, was significantly decreased in *Ogr1*^{-/-} grafts at day 7 compared to WT grafts (*Tgfb1*: 2.33 ± 0.47 (n=11) vs. 4.75 ± 0.94 (n=7) $**P < 0.01$, Figure 4C. *Ctgf*: 3.12 ± 0.59 (n=10) vs. 8.08 ± 2.63 , (n=7) $*P < 0.05$, Figure 4D). In summary, markers of fibrogenesis are significantly decreased in *Ogr1*^{-/-} grafts compared to WT grafts in this heterotopic transplantation model for intestinal fibrosis. Fibrosis was successfully induced in this model in the WT grafts, whereas the expression of fibrosis markers remained unchanged in the *Ogr1*^{-/-} grafts after heterotopic transplantation.

Collagen deposition is decreased in *Ogr1*^{-/-} grafts after induction of fibrosis

Collagen layer thickness visualized by Sirius red staining was quantified under transmission light and under polarizing light before and after induction of fibrosis

(Figure 5). Collagen deposition was increased when using terminal ileum from WT mice as grafts (collagen layer thickness $12.44 \pm 0.51 \mu\text{m}$ (n=8) vs. $8.72 \pm 0.68 \mu\text{m}$ (n=6), *** $P < 0.001$ under transmission light (Figure 5A), $10.71 \pm 0.41 \mu\text{m}$ (n=8) vs. $6.80 \pm 0.38 \mu\text{m}$ (n=6), *** $P < 0.001$ under polarized light (Figure 5B)). Consistent with the increase in the mRNA expression of fibrosis markers, the collagen layer in the *Ogr1*^{-/-} grafts was significantly increased 7 days after heterotopic transplantation (collagen layer thickness $10.56 \pm 0.29 \mu\text{m}$ (n=11) vs. $7.93 \pm 0.47 \mu\text{m}$ (n=6), ** $P < 0.01$ under transmission light (Figure 5A), $8.71 \pm 0.39 \mu\text{m}$ (n=11) vs. $5.91 \pm 0.31 \mu\text{m}$ (n=6), *** $P < 0.001$ under polarized light (Figure 5B)). Consistent with expression of the fibrosis mRNA, the collagen layer in harvested grafts at day 7 from *Ogr1*^{-/-} mice was significantly thinner compared to the collagen layer in grafts from WT mice ($10.56 \pm 0.29 \mu\text{m}$ (n=11) vs. $12.44 \pm 0.51 \mu\text{m}$ (n=8), ** $P < 0.01$ for data obtained under transmission light (Figure 5A) and $8.71 \pm 0.39 \mu\text{m}$ (n=11) vs. $10.71 \pm 0.41 \mu\text{m}$ (n=8), *** $P < 0.001$ for data obtained under polarized light microscopy (Figure 5B)).

Collagen deposition in the grafts was furthermore quantified by image processing evaluation (color threshold) with ImageJ. Polarized light microscopy showed a significant decrease in collagen layer thickness in grafts from *Ogr1*^{-/-} donor mice compared to grafts from WT donor mice (0.44 ± 0.06 (n=11) vs. 0.73 ± 0.10 (n=8), arbitrary units, * $P < 0.05$ (Figure 5C)).

HYP content is significantly decreased in *Ogr1*^{-/-} grafts

Formation of HYP, an amino acid playing a key role in the stability of collagen, was determined in explanted grafts from mice at day 7 after heterotopic transplantation. HYP content was significantly decreased in grafts from *Ogr1*^{-/-}

donor mice compared to grafts of WT donor mice after heterotopic transplantation (0.12 ± 0.02 (n=9) vs. 0.31 ± 0.04 (n=4), $***P < 0.001$, Figure 6). This result confirms that collagen deposition, as well as collagen stability is reduced upon *Ogr1* depletion in this murine model of intestinal fibrosis.

Heat shock protein 90B1 (HSP90B1) decreases in *Ogr1*^{-/-} grafts upon induction of fibrosis

mRNA expression of the stress-associated gene HSP90B1 decreased significantly in grafts from *Ogr1*^{-/-} donor mice at day 7 after heterotopic transplantation compared to day 0 (0.25 ± 0.06 (n=11) vs. 1.04 ± 0.21 (n=6) respectively, $***P < 0.001$, Supplementary figure 3). A trend towards a decreased HSP90B1 mRNA expression was observed in grafts from WT donor mice after transplantation compared to day 0.

DISCUSSION

In the present study we aimed to determine whether the pH-sensing receptor OGR1 plays a role in fibrosis in the terminal ileum. When analyzing the terminal ileum from patients with CD, we observed increased expression of the pH-sensing GPRs *OGR1* (*GPR68*), *TDAG8* (*GPR65*) and *GPR4* in the fibrosis-affected area, compared to the non-fibrotic resection margin. We also found a positive correlation between the expression of markers involved in different phases of fibrosis, e.g. pro-fibrotic cytokines (*TGFB1* and *CTGF*), a marker for activation of myofibroblasts (*ACTA2*) or pro-collagens (*COL1A1* and *COL3A1*), and the expression of *OGR1* (*GPR68*), *TDAG8* (*GPR65*) and *GPR4*. Using a well-established *in vivo* murine model for intestinal fibrosis, we could confirm an increased expression of the pH-sensing receptors *Ogr1* (*Gpr68*) and *Tdag8* (*Gpr65*) upon fibrogenesis. Furthermore, comparing heterotopic transplantation of terminal ileum from *Ogr1*^{-/-} mice to transplantation of ileum from WT mice, we detected a significant decrease in the mRNA expression of fibrosis markers, as well as a decrease in collagen layer thickness and HYP in the *Ogr1*^{-/-} grafts. These results indicate a role for the pH-sensing receptor OGR1 in fibrogenesis and stricture formation in CD, thereby providing a new target for therapeutic intervention.

Intestinal fibrosis, which typically occurs in the terminal ileum of patients with CD, is triggered as a response to inflammatory processes, in which fibroblasts become activated. Activated myofibroblasts can deposit excessive amounts of ECM proteins as part of the wound healing process, thereby causing stricture formation.⁴⁰ Fibrosis is the result of a disturbance in the balance between ECM formation and matrix metalloproteinase mediated degradation of ECM

proteins.⁴¹ It is widely accepted that intestinal inflammation is accompanied by tissue acidification due to the hypoxic environment and the excessive production and insufficient elimination of glycolytic metabolites e.g. lactic acid.⁴²⁻⁴⁴ Local acidification of the gut lumen as well as the gut mucosa during intestinal inflammation has been described. This indicates that luminal and tissue pH is decreased during active and longstanding IBD, which could activate down-stream signaling by pH-sensing receptors. The heterotopic transplantation of intestine resections under the skin induces a cellular, fibrosis-inducing response from the graft as well as from the recipient.³⁸ The graft is subjected to ischemia, which causes hypoxia and thereby anaerobic glycolysis and production of lactic acid.¹⁴⁻¹⁶ The ensuing decrease in pH may stimulate pH-sensing receptors such as OGR1. Furthermore, hypoxia induces the accumulation of hypoxia-inducible-factors (HIFs) and the release of pro-inflammatory cytokines such as TNF and interleukin (IL) 6.^{45, 46} Only recently we found that the pH-sensing receptor OGR1 plays a role in IBD and that genetic deletion of *Ogr1* partially prevents the development of colitis in the *IL10* deficient IBD mouse model.⁴ Moreover, the absence of *Gpr4* ameliorates colitis in IBD animal models indicating an important regulatory role of this pH-sensing receptor in mucosal inflammation.⁵ Recently, we showed that expression of *Ogr1*, *Tdag8*, *Il6* and *Tnf* is induced by the combination of hypoxia and extracellular acidosis in WT mouse peritoneal macrophages, but not in peritoneal macrophages from *Ogr1*^{-/-} mice.⁴⁶ Taken together, these studies indicate a pathophysiological role for pH-sensing receptors during the pathogenesis of mucosal inflammation, and provide a new link between tissue pH and immune responses.⁴

pH-sensing is not only relevant for the induction of inflammation, but also for the progression of fibrosis. Links between extra-cellular acidification and activation of fibroblasts, as well as ECM remodeling via GPRs have been described before. Zhu *et al.* demonstrated that differentiation of human bone-marrow derived mesenchymal stem cells (MSCs) into cancer-associated fibroblasts via OGR1, occurs upon decreasing the extracellular pH to 7.0 *in vitro*. In this study, differentiation of MSCs into myofibroblasts was accompanied by increased protein expression of vimentin and alpha smooth muscle actin (α SMA).⁴⁷ Furthermore, Li *et al.* show that migration of MCF-7 cells (human breast adenocarcinoma cell line) over-expressing OGR1 is decreased (without exposing them to an acidic environment) and that this effect might be mediated via a GTPase G α 12/13- Rho-Rac1 pathway.⁴⁷ Differences in migratory function of intestinal fibroblasts isolated from stricturing and fistulating areas upon activation have been determined as factors in the mechanism of intestinal fibrosis as well. These mechanisms may contribute to the induction of fibrosis in this model, and explain the reduced fibrotic processes in grafts from *Ogr1*^{-/-} mice.⁴⁸

OGR1 is also involved in tissue remodeling in severe asthma and irreversible airway obstruction.⁴⁹ Airway remodeling results from increased expression of connective tissue or extracellular matrix proteins, airway smooth muscle cells (ASMC) hyperplasia, and hypertrophy,⁵⁰ and is associated with airway acidification in asthma.⁵¹ The extracellular acidic pH-induced effects, like the induction of connective tissue growth factor expression, can be inhibited by inhibiting OGR1 with small interfering RNA and protein-specific inhibitors.⁴⁹ Further, Saxena *et al.* described that activation of *OGR1* in human (ASMC) by

decreasing the extracellular pH to 6.8 causes contraction and cell stiffness, which was attenuated by *OGR1* silencing.⁵²

There is evidence that intestinal fibrogenesis is self-perpetuating,⁵³ and that once initiated, its progression might no longer depend on the presence of inflammation but could depend on persisting mucosal acidification.⁵⁴ Administration of anti-inflammatory agents effectively treats inflammatory flares, but may not prevent intestinal fibrosis.^{55, 56}

In conclusion, we provide the first evidence that OGR1 plays a role in intestinal fibrosis. *Ogr1* deficiency leads to a significant decrease in mRNA expression of fibrosis markers, as well as an evident reduction in collagen deposition in our model for intestinal fibrosis. A decrease in HYP content after induction of fibrosis points to that also stabilization of collagen is impaired in grafts from *Ogr1*^{-/-} compared to WT. The relevance of these findings is expanded by the positive correlation between the expression of GPRs and fibrosis markers in human ileum affected with fibrosis in CD patients. Increased expression of OGR1 triggered by inflammation-associated acidification, and subsequent cellular responses might perpetuate inflammation-induced fibrosis in IBD. The presence of OGR1 in human and murine intestinal tissue is associated with fibrosis making it a potential future target for treatment against IBD associated fibrogenesis.

FUNDING

This research was supported by a research grant FreeNovation from Novartis to MH, by a research grant [grant number: 314730_152895 / 1] from

the Swiss National Science Foundation to MH and by a grant from the Swiss National Science Foundation [grant number 31003A_155959] to CAW.

GR discloses grant support from AbbVie, Ardeypharm, MSD, FALK, Flamentera, Novartis, Roche, Tillots, UCB and Zeller. MH discloses grant support from AbbVie and Novartis. GD discloses unrestricted grants: Abbvie, Takeda, Advisory boards: Mundipharma, Pharmacosmos, Speakers fee: Takeda, Janssen pharmaceuticals. SH, WTVH, AH, KB, TR, CM, BM, BW, CM, CdV, AW, CAW, IFW and PAR have no conflict of interest to disclose.

REFERENCES

1. Franke A, McGovern DP, Barrett JC, et al. Genome-wide meta-analysis increases to 71 the number of confirmed Crohn's disease susceptibility loci. *Nature genetics* 2010;42(12):1118-25.
2. Jostins L, Ripke S, Weersma RK, et al. Host-microbe interactions have shaped the genetic architecture of inflammatory bowel disease. *Nature* 2012;491(7422):119-24.
3. de Valliere C, Vidal S, Clay I, et al. The pH-sensing receptor OGR1 improves barrier function of epithelial cells and inhibits migration in an acidic environment. *American journal of physiology Gastrointestinal and liver physiology* 2015;309(6):G475-90.
4. de Valliere C, Wang Y, Eloranta JJ, et al. G Protein-coupled pH-sensing Receptor OGR1 Is a Regulator of Intestinal Inflammation. *Inflammatory bowel diseases* 2015;21(6):1269-81.
5. Wang Y, de Valliere C, Imenez Silva PH, et al. The proton-activated receptor GPR4 modulates intestinal inflammation. *Journal of Crohn's & colitis* 2017
6. Seuwen K, Ludwig MG, Wolf RM. Review - Receptors for protons or lipid messengers or both? *J Recept Sig Transd* 2006;26(5-6):599-610.
7. Ludwig MG, Vanek M, Guerini D, et al. Proton-sensing G-protein-coupled receptors. *Nature* 2003;425(6953):93-8.
8. Venkatakrisnan AJ, Deupi X, Lebon G, et al. Molecular signatures of G-protein-coupled receptors. *Nature* 2013;494(7436):185-94.

-
- 535 9. Heng BC, Aubel D, Fussenegger M. An overview of the diverse roles of G-
536 protein coupled receptors (GPCRs) in the pathophysiology of various
537 human diseases. *Biotechnol Adv* 2013;31(8):1676-94.
- 538 10. Chini B, Parenti M, Poyner DR, et al. G-Protein-Coupled Receptors: from
539 Structural Insights to Functional Mechanisms. *Biochem Soc T*
540 2013;41:135-36.
- 541 11. Wang JQ, Kon J, Mogi C, et al. TDAG8 is a proton-sensing and psychosine-
542 sensitive G-protein-coupled receptor. *J Biol Chem* 2004;279(44):45626-
543 33.
- 544 12. Ishii S, Kihara Y, Shimizu T. Identification of T cell death-associated gene
545 8 (TDAG8) as a novel acid sensing G-protein-coupled receptor. *J Biol*
546 *Chem* 2005;280(10):9083-87.
- 547 13. Mogi C, Tobo M, Tomura H, et al. Involvement of Proton-Sensing TDAG8
548 in Extracellular Acidification-Induced Inhibition of Proinflammatory
549 Cytokine Production in Peritoneal Macrophages. *J Immunol*
550 2009;182(5):3243-51.
- 551 14. Park SY, Bae DJ, Kim MJ, et al. Extracellular low pH modulates
552 phosphatidylserine-dependent phagocytosis in macrophages by
553 increasing stabilin-1 expression. *The Journal of biological chemistry*
554 2012;287(14):11261-71.
- 555 15. Simmen HP, Battaglia H, Giovanoli P, et al. Analysis of pH, pO₂ and pCO₂
556 in drainage fluid allows for rapid detection of infectious complications
557 during the follow-up period after abdominal surgery. *Infection*
558 1994;22(6):386-9.

-
- 559 16. Lardner A. The effects of extracellular pH on immune function. *J Leukoc*
560 *Biol* 2001;69(4):522-30.
- 561 17. Hanly EJ, Aurora AA, Shih SP, et al. Peritoneal acidosis mediates
562 immunoprotection in laparoscopic surgery. *Surgery* 2007;142(3):357-64.
- 563 18. Brokelman WJ, Lensvelt M, Borel Rinkes IH, et al. Peritoneal changes due
564 to laparoscopic surgery. *Surg Endosc* 2011;25(1):1-9.
- 565 19. Mohebbi N, Benabbas C, Vidal S, et al. The proton-activated G protein
566 coupled receptor OGR1 acutely regulates the activity of epithelial proton
567 transport proteins. *Cell Physiol Biochem* 2012;29(3-4):313-24.
- 568 20. Pardo A, Selman M. Matrix metalloproteases in aberrant fibrotic tissue
569 remodeling. *Proc Am Thorac Soc* 2006;3(4):383-8.
- 570 21. Kim H, Oda T, Lopez-Guisa J, et al. TIMP-1 deficiency does not attenuate
571 interstitial fibrosis in obstructive nephropathy. *J Am Soc Nephrol*
572 2001;12(4):736-48.
- 573 22. Underwood DC, Osborn RR, Bochnowicz S, et al. SB 239063, a p38 MAPK
574 inhibitor, reduces neutrophilia, inflammatory cytokines, MMP-9, and
575 fibrosis in lung. *Am J Physiol Lung Cell Mol Physiol* 2000;279(5):L895-
576 902.
- 577 23. Vaillant B, Chiaramonte MG, Cheever AW, et al. Regulation of hepatic
578 fibrosis and extracellular matrix genes by the Th response: new insight
579 into the role of tissue inhibitors of matrix metalloproteinases. *J Immunol*
580 2001;167(12):7017-26.
- 581 24. Specia S, Giusti I, Rieder F, et al. Cellular and molecular mechanisms of
582 intestinal fibrosis. *World J Gastroenterol* 2012;18(28):3635-61.

-
- 583 25. Rieder F, Fiocchi C, Rogler G. Mechanisms, Management, and Treatment
584 of Fibrosis in Patients With Inflammatory Bowel Diseases.
585 *Gastroenterology* 2017;152(2):340-50 e6.
- 586 26. Latella G, Di Gregorio J, Flati V, et al. Mechanisms of initiation and
587 progression of intestinal fibrosis in IBD. *Scandinavian journal of*
588 *gastroenterology* 2015;50(1):53-65.
- 589 27. Latella G, Rogler G, Bamias G, et al. Results of the 4th scientific workshop
590 of the ECCO (I): Pathophysiology of intestinal fibrosis in IBD. *Journal of*
591 *Crohn's & colitis* 2014
- 592 28. Lawrance IC, Rogler G, Bamias G, et al. Cellular and Molecular Mediators
593 of Intestinal Fibrosis. *J Crohns Colitis* 2015
- 594 29. Li C, Flynn RS, Grider JR, et al. Increased activation of latent TGF-beta1
595 by alphaVbeta3 in human Crohn's disease and fibrosis in TNBS colitis
596 can be prevented by cilengitide. *Inflammatory bowel diseases*
597 2013;19(13):2829-39.
- 598 30. Li C, Iness A, Yoon J, et al. Noncanonical STAT3 activation regulates
599 excess TGF-beta1 and collagen I expression in muscle of stricturing
600 Crohn's disease. *Journal of immunology* 2015;194(7):3422-31.
- 601 31. Scarpa M, Bortolami M, Morgan SL, et al. TGF-beta1 and IGF-1 and
602 anastomotic recurrence of Crohn's disease after ileo-colonic resection.
603 *Journal of gastrointestinal surgery : official journal of the Society for*
604 *Surgery of the Alimentary Tract* 2008;12(11):1981-90.
- 605 32. Del Zotto B, Mumolo G, Pronio AM, et al. TGF-beta1 production in
606 inflammatory bowel disease: differing production patterns in Crohn's

- 607 disease and ulcerative colitis. *Clinical and experimental immunology*
608 2003;134(1):120-6.
- 609 33. de Bruyn JR, Meijer SL, Wildenberg ME, et al. Development of Fibrosis in
610 Acute and Longstanding Ulcerative Colitis. *Journal of Crohn's & colitis*
611 2015;9(11):966-72.
- 612 34. Cosnes J, Cattan S, Blain A, et al. Long-term evolution of disease behavior
613 of Crohn's disease. *Inflammatory bowel diseases* 2002;8(4):244-50.
- 614 35. Freeman HJ. Natural history and clinical behavior of Crohn's disease
615 extending beyond two decades. *J Clin Gastroenterol* 2003;37(3):216-9.
- 616 36. Ippolito C, Colucci R, Segnani C, et al. Fibrotic and Vascular Remodelling
617 of Colonic Wall in Patients with Active Ulcerative Colitis. *J Crohns Colitis*
618 2016
- 619 37. Grossmann J, Walther K, Artinger M, et al. Progress on isolation and short-
620 term ex-vivo culture of highly purified non-apoptotic human intestinal
621 epithelial cells (IEC). *European journal of cell biology* 2003;82(5):262-
622 70.
- 623 38. Hausmann M, Rechsteiner T, Caj M, et al. A New Heterotopic Transplant
624 Animal Model of Intestinal Fibrosis. *Inflammatory bowel diseases* 2013
- 625 39. Rittie L. Method for Picrosirius Red-Polarization Detection of Collagen
626 Fibers in Tissue Sections. *Methods in molecular biology (Clifton, NJ)*
627 2017;1627:395-407.
- 628 40. M. P. Fibrosis in the GI tract: pathophysiology, diagnosis and treatment
629 options. *Front Gastrointest Res* 2010;26:15-31.
- 630 41. van Haaften WT, Mortensen JH, Karsdal MA, et al. Misbalance in type III
631 collagen formation/degradation as a novel serological biomarker for

- 632 penetrating (Montreal B3) Crohn's disease. *Aliment Pharmacol Ther*
633 2017;46(1):26-39.
- 634 42. Fallingborg J, Christensen LA, Jacobsen BA, et al. Very low intraluminal
635 colonic pH in patients with active ulcerative colitis. *Dig Dis Sci*
636 1993;38(11):1989-93.
- 637 43. Nugent SG, Kumar D, Rampton DS, et al. Intestinal luminal pH in
638 inflammatory bowel disease: possible determinants and implications for
639 therapy with aminosalicylates and other drugs. *Gut* 2001;48(4):571-7.
- 640 44. Press AG, Hauptmann IA, Hauptmann L, et al. Gastrointestinal pH profiles
641 in patients with inflammatory bowel disease. *Aliment Pharmacol Ther*
642 1998;12(7):673-8.
- 643 45. Bartels K, Grenz A, Eltzschig HK. Hypoxia and inflammation are two sides
644 of the same coin. *Proc Natl Acad Sci U S A* 2013;110(46):18351-2.
- 645 46. de Valliere C, Cosin-Roger J, Simmen S, et al. Hypoxia Positively Regulates
646 the Expression of pH-Sensing G-Protein-Coupled Receptor OGR1
647 (GPR68). *Cell Mol Gastroenterol Hepatol* 2016;2(6):796-810.
- 648 47. Zhu H, Guo S, Zhang Y, et al. Proton-sensing GPCR-YAP Signalling
649 Promotes Cancer-associated Fibroblast Activation of Mesenchymal
650 Stem Cells. *Int J Biol Sci* 2016;12(4):389-96.
- 651 48. Meier JK, Scharl M, Miller SN, et al. Specific differences in migratory
652 function of myofibroblasts isolated from Crohn's disease fistulae and
653 strictures. *Inflammatory bowel diseases* 2011;17(1):202-12.
- 654 49. Matsuzaki S, Ishizuka T, Yamada H, et al. Extracellular acidification induces
655 connective tissue growth factor production through proton-sensing

- 656 receptor OGR1 in human airway smooth muscle cells. *Biochem Biophys*
657 *Res Commun* 2011;413(4):499-503.
- 658 50. Vignola AM, Kips J, Bousquet J. Tissue remodeling as a feature of
659 persistent asthma. *J Allergy Clin Immunol* 2000;105(6 Pt 1):1041-53.
- 660 51. Kodric M, Shah AN, Fabbri LM, et al. An investigation of airway acidification
661 in asthma using induced sputum: a study of feasibility and correlation.
662 *American journal of respiratory and critical care medicine*
663 2007;175(9):905-10.
- 664 52. Saxena H, Deshpande DA, Tiegs BC, et al. The GPCR OGR1 (GPR68)
665 mediates diverse signalling and contraction of airway smooth muscle in
666 response to small reductions in extracellular pH. *Br J Pharmacol*
667 2012;166(3):981-90.
- 668 53. Johnson LA, Luke A, Sauder K, et al. Intestinal fibrosis is reduced by early
669 elimination of inflammation in a mouse model of IBD: impact of a "Top-
670 Down" approach to intestinal fibrosis in mice. *Inflammatory bowel*
671 *diseases* 2012;18(3):460-71.
- 672 54. Rieder F, Kessler S, Sans M, et al. Animal models of intestinal fibrosis: new
673 tools for the understanding of pathogenesis and therapy of human
674 disease. *Am J Physiol Gastrointest Liver Physiol* 2012;303(7):G786-801.
- 675 55. D'Haens G, Geboes K, Rutgeerts P. Endoscopic and histologic healing of
676 Crohn's (ileo-) colitis with azathioprine. *Gastrointestinal endoscopy*
677 1999;50(5):667-71.
- 678 56. Vermeire S, van Assche G, Rutgeerts P. Review article: Altering the natural
679 history of Crohn's disease--evidence for and against current therapies.
680 *Alimentary pharmacology & therapeutics* 2007;25(1):3-12.

FIGURE LEGENDS

Figure 1: mRNA expression of fibrosis markers *COL1A1*, *COL3A1*, *ACTA2*, *TGFB1* (A) and G-protein coupled receptors (GPRs) *OGR1* (*GPR68*), *TDAG8* (*GPR65*), *GPR4* and *GPR132* (B) in fibrotic versus non-fibrotic terminal ileum of patients with CD (by Wilcoxon matched-pairs signed rank test).

Figure 2: Positive correlation in mRNA expression between *OGR1* (*GPR68*) vs. *COL3A1* (R^2 0.791, $P < 0.001$) and *TGFB1* (R^2 0.791, $P < 0.01$) (by Spearman's rank correlation coefficient).

Figure 3: *Ogr1* (*Gpr68*, A) (by unpaired t-test) and *Tdag8* (*Gpr65*, B) (by ANOVA post-hoc Newman-Keuls multiple comparison test) mRNA expression is significantly increased in WT grafts explanted 7 days after heterotopic transplantation. *Tdag8* (*Gpr65*) mRNA expression is significantly decreased in grafts from *Ogr1*^{-/-} donor mice at day 7 compared to grafts from WT donor mice at day 7.

Figure 4: *Vim* (A), *Col3a1* (B), *Tgfb1* (C) and *Ctgf* (D) mRNA expression is significantly decreased in grafts from *Ogr1*^{-/-} mice 7 days after heterotopic transplantation compared to WT grafts (ANOVA post-hoc Newman-Keuls multiple comparison test).

Figure 5: Collagen quantity and collagen layer thickness are significantly decreased in grafts from *Ogr1*^{-/-} donor mice compared to WT donor mice 7 days after heterotopic transplantation. Quantification of collagen layer thickness (μm) by Sirius red staining with and without polarized light filter (A+B, by ANOVA post-hoc Newman-Keuls multiple comparison test). Area of collagen deposition stained by Sirius Red and quantified using ImageJ under transmission light (C).

Representative pictures of collagen deposition visualized using Sirius red staining with and without polarized light (D).

Figure 6: HYP content is decreased in grafts from *Ogr1*^{-/-} donor mice explanted at day 7 after heterotopic transplantation compared to grafts from WT donor mice (by unpaired t-test).

Supplementary figure 1: mRNA expression of fibrosis markers COL1A1, COL3A1, ACTA2, TGFB1 (A) and G-protein coupled receptors (GPRs) OGR1 (GPR68), TDAG8 (GPR65) GPR4 and GPR132 (B) in non-fibrotic terminal ileum of patients with CD compared to non-cancer affected terminal ileum of patients with colonic adenocarcinoma (by Mann-Whitney U test rank test).

Supplementary figure 2: *GPR68* (*OGR1*), *GPR65* (*TDAG8*), *GPR132* and *GPR4* mRNA expression in whole human intestinal mucosa is significantly increased compared to the expression in isolated intestinal crypts (by Kruskal-Wallis post-hoc Dunn's multiple comparison).

Supplementary figure 3: *Hsp90b1* mRNA expression is significantly decreased in *Ogr1*^{-/-} grafts 7 days after heterotopic transplantation compared to day 0 (**p < 0.001 by ANOVA post-hoc Newman-Keuls multiple comparison test).

TABLES

Table 1		OGR1 (GPR68)	TDAG8 (GPR65)	GPR4	GPR132
COL1A1	Correlation				
	Coefficient	0.791	0.783	0.887	0.036
	P value	0.000	0.000	0.000	0.880
COL3A1	Correlation				
	Coefficient	0.779	0.764	0.905	0.006
	P value	0.000	0.000	0.000	0.980
ACTA2	Correlation				
	Coefficient	0.689	0.782	0.880	-0.120
	P value	0.001	0.000	0.000	0.613
TGFB1	Correlation				
	Coefficient	0.850	0.913	0.820	0.137
	P value	0.000	0.000	0.000	0.565
OGR1 (GPR68)	Correlation				
	Coefficient		0.898	0.758	0.869
	P value		0.000	0.000	0.000

Table 1: Spearman correlation between markers for fibrosis and G-protein coupled receptors (GPRs).

726 SUPPLEMENTARY TABLES

	CD (n=8)	Control (n=4)
General		
Gender, % female	8 (100%)	2 (50%)
Age at sample, years (mean, min-max)	34.7 (21.1-65.6)	73.1 (69.1-78.2)
Disease duration, years, (mean, min-max)	8.6 (0.8-35.2)	NA
Montreal age at diagnosis (n (%))		
17-40 years (A2)	8 (100%)	NA
Montreal disease behavior (n (%))		
Stricturing disease (B2)	8 (100%)	NA
Disease location (n (%))		
Terminal ileum (L1)	4 (50%)	NA
Ileocolon (L3)	4 (50%)	
C-reactive protein before operation (n (%))		
C-reactive protein >5mg/L	2 (25%)	NA
C-reactive protein <5mg/L	4 (50%)	
Missing	2 (25%)	
Clinical disease activity before operation (n (%))		
Disease in remission	0 (0%)	NA
Mild disease	1 (12.5%)	
Moderate disease	4 (50%)	
Severe disease	3 (37.5%)	
Medication (n (%))		
No medication	1 (12.5%)	NA
Corticosteroids	1 (12.5%)	
Azathioprine/6-mercaptopurine	2 (25%)	
Azathioprine/6-mercaptopurine + corticosteroids	2 (25%)	
Anti-TNF	1 (12.5%)	
Anti-IL12/23 + corticosteroids	1 (12.5%)	

727 Supplementary Table 1: Characteristics of patients with CD and control

728 patients. CD: Crohn's disease, NA: Not applicable

Gene	Full name	Taqman expression ID
Human		
<i>GPR68</i>	Ovarian cancer G-protein coupled receptor-1	Hs00268858_s1
<i>GPR65</i>	T cell death-associated gene 8	Hs00269247_s1
<i>GPR4</i>	G-protein coupled receptor 4	Hs00270999_s1
<i>GPR132</i>	G-protein coupled receptor 132	Hs01871869_s1
<i>COL1A1</i>	Pro-collagen type III alpha 1	Hs00164004_m1
<i>COL3A1</i>	Pro-collagen type I alpha 1	Hs00943809_m1
<i>ACTA2</i>	α -smooth muscle actin	Hs00426835_g1
<i>TGFB1</i>	Transforming growth factor beta 1	Hs00998133_m1
<i>HPRT</i>	Hypoxanthine phosphoribosyltransferase 1	4326321E
<i>ACTB</i>	Beta-actin	4310881E
<i>GAPDH</i>	Glyceraldehyde-3-phosphate dehydrogenase	4326317E
Murine		
<i>Gpr68</i>	Ovarian cancer G-protein coupled receptor-1	Mm00558545_s1
<i>Gpr65</i>	T cell death-associated gene 8	Mm00433695_m1
<i>Tgfb1</i>	Transforming growth factor beta 1	Mm01178820_m1
<i>Vim</i>	Vimentin	Mm01333430_m1
<i>Hsp90b1</i>	Heat shock protein 90, beta (Grp94) member 1	Mm00441926_m1
<i>Ctgf</i>	Connective tissue growth factor	Mm01192933_g1
<i>Col3a1</i>	Pro-collagen type III alpha 1	Mm01254476_m1
<i>Gapdh</i>	Glyceraldehyde-3-phosphate dehydrogenase	4352339E

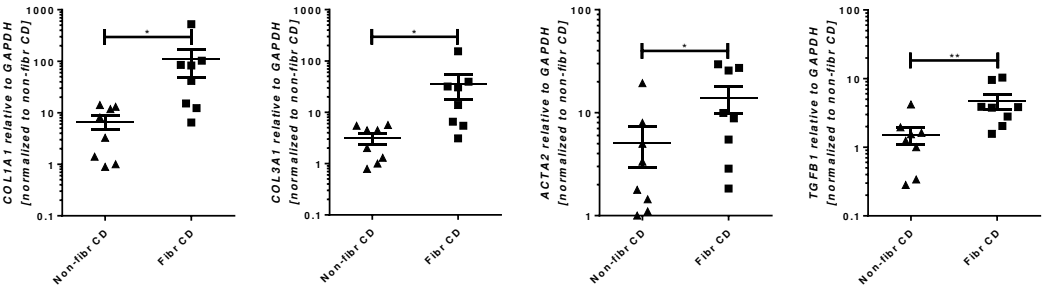
Supplementary Table 2: Taqman gene expression assays

729

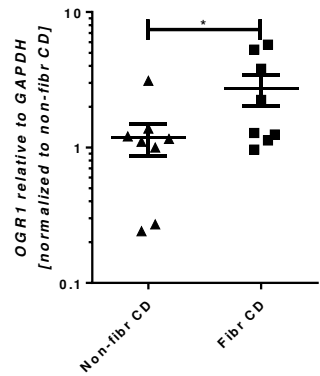
730

Figure 1

A



B



C

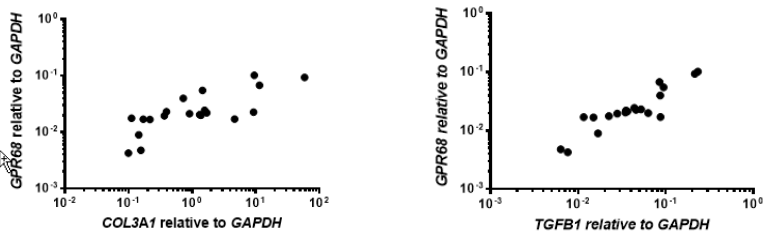
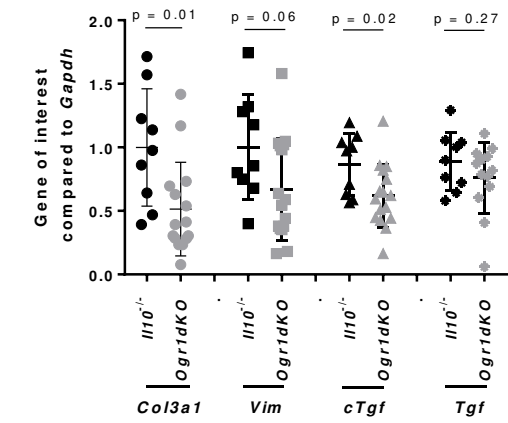
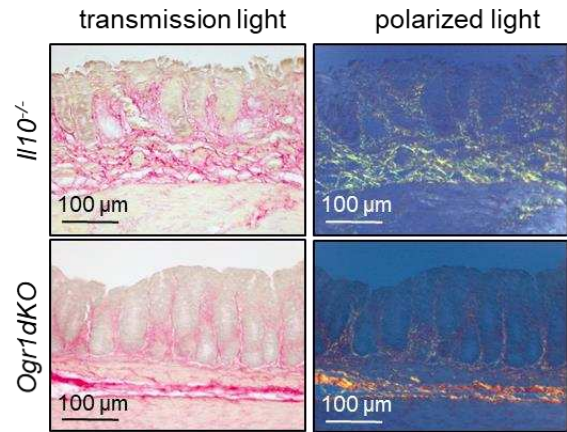


Figure 2

A



B



C

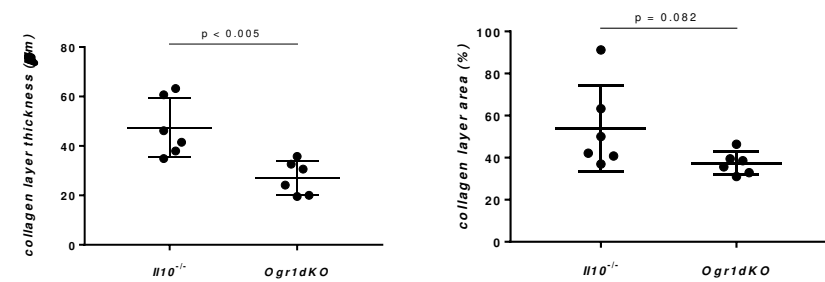


Figure 3

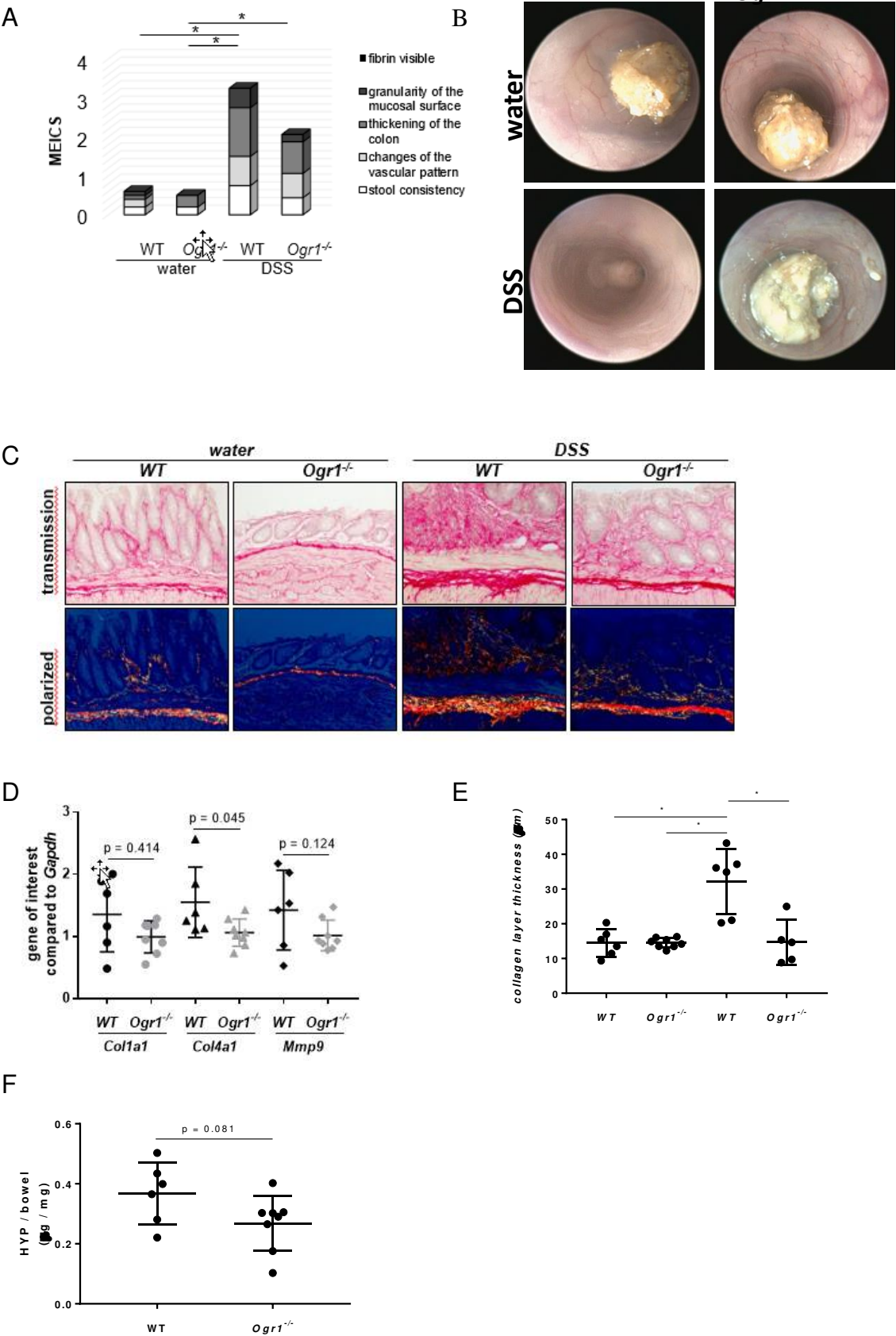


Figure 4

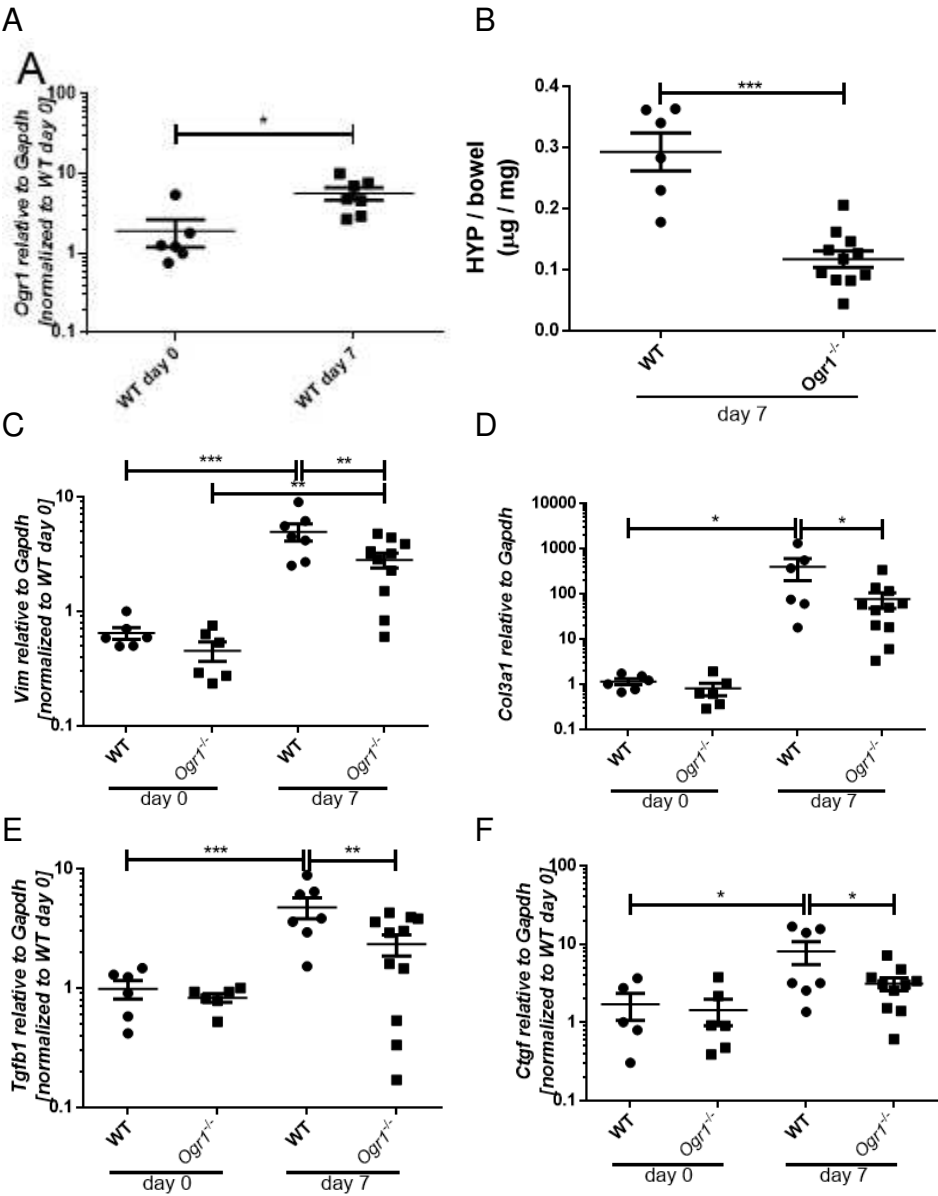


Figure 5

